Journal of Materials Chemistry B

Accepted Manuscript

ROYAL SOCIETY OF CHEMISTRY

www.rsc.org/materialsB

Cetirizine derived supramolecular topical gel in action: rational design, characterization and *in vivo* self-delivery application in treating skin allergy in mice

Joydeb Majumder,[a] Jolly Deb,[b] Ahmad Husain, [a] Siddhartha Sankar Jana,[b,*] and Parthasarathi Dastidar [a,*]

[a] Department of Organic Chemistry, Indian Association for the Cultivation of Science,

2A & 2B Raja S. C. Mullick Road, Kolkata-700032, India.

[b] Department of Biological Chemistry, Indian Association for the Cultivation of Science,

2A & 2B Raja S. C. Mullick Road, Kolkata-700032, India.

* Corresponding author. Tel.: +91 33 2473 4971; Fax: +91 33 2473 2805

E-mail addresses: ocpd@iacs.res.in, bcssj@iacs.res.in

Abstract

Conventional drug delivery system requires a delivery vehicle which often faces various problems such as inefficient drug loading into the delivery vehicle and its release, cytotoxicity and biodegradability of the delivery vehicle etc., whereas supramolecular gel based self-delivery system delivers a gelator drug at the target site without using any vehicle thereby getting rid of such problems. Here, a simple salt formation strategy has been employed to convert a well known anti-allergic drug (cetirizine) to a supramolecular gelator for the purpose of making a topical gel for *in vivo* self-delivery applications. The salt of cetirizine and tyramine (salt **3**) displays excellent gelation property in methylsalicylate/menthol. The gels are characterised by electron microscopy, table top- and dyanamic rheology. The gelator salt **3** displays excellent physiological stability in phosphate buffer saline (PBS) and it is biocompatible in mouse macrophage RAW 264.7 and mouse myoblast C2C12 cell lines. A methylsalicylate/menthol topical gel of salt **3** is successfully self-delivered in treating 2, 4–dinitro chloro benzene (DNCB)–induced allergic skin condition in mice.

1. Introduction

The main objective of the present study is to develop anti-allergic drug based supramolecular topical gel for self-delivery applications. In self-delivery system, a drug or prodrug or bioactive molecule itself is converted to a gelator and delivered at the target site in the form of supramolecular gel. The need for self-delivery system in drug delivery research arises because of the usual impediments associated with the conventional drug delivery wherein a carrier or vehicle molecule (usually a polymer) is needed; biostability, biodegradability, cytotoxicity of the carrier molecules, and drug loading and its release etc.[1,2] are the major challenges in developing such drug delivery systems. On the other hand, no such drug

delivery vehicle (carrier molecule) is needed in self-delivery system thereby making it technologically more advanced. In recent years much impetus has been given towards the developing of supramolecular gel based self-delivery systems.[3-7]

Supramolecular gels are visco-elastic materials comprising of a liquid phase immobilized within a three dimensional network generated from the self-assembly of gelator molecules driven by various non-covalent interactions such as hydrogen bonding, π–π stacking, donor–acceptor interactions, metal coordination, van der Waals interactions etc. Small molecules (MW < 3000) capable of hardening (gelling) various organic and aqueous fluids are known as low molecular weight gelators (LMWGs).[8-13] The gelator molecules first self assemble to form various supramolecular architectures such as 1D fibers, rods, helices etc. which further entangle to form 3D - self-assembled fibrillar networks (SAFiNs)[14] within which the solvent molecules are trapped to form gel. Depending on the gelling solvents, the resulting gel is termed organogel (organic solvent) or hydrogel (pure water or aqueous solvents). Over the decades, LMWGs attracted much attention due to their various potential applications such as in electro-optics/photonics,[15] sensors,[16,17] cosmetics,[18] structure-directing agents[19] etc. Some gels are also used as reaction media for catalysis,[20] in conservation of art[21] etc. Supramolecular gels have also been explored for developing biomaterials for various biomedical applications such as tissue engineering,[22] biomineralization,[23] wound healing,[24] medical diagnostics,[25] drug delivery,[26-28] enzyme mimics,[29] inhibitors of cancer cells,[30] 3D cell cultures[31] etc. However, the design of new gelators is a challenging task because of the lack of molecular-level understanding of the gel-forming mechanism; nevertheless, there are some significant efforts by different groups in designing new LMWGs.[32-41]

One such early report was by Shinkai et al.; the study based on the single crystal structures of sugar derivatives concluded that 1D hydrogen bonded network (HBN) promoted gelation whereas 0D or 2D HBN either produced weak gel or no gelation at al.[42] We have been

exploiting the 1D HBN forming supramolecular synthons[43] in the context of crystal engineering[44] in designing organic-salt-based gelators.[45-47] The salt based supramolecular gelators we reported thus far are technologically advantageous since salt formation is the easiest reaction to carry out with quantitative or near quantitative yield allowing preparation of a large number and quantity of salts within a short period of time to facilitate efficient gelation screening. Moreover the charge assisted hydrogen bond in salts is stronger (40-190 kJ mol^{-1}) than that of the normal hydrogen bond (10-65 kJ mol^{-1}) and also directional making the material more robust – an important criterion for material applications. The goal of this work was to design drug based supramolecular gelator following salt formation rationale. In the present study, we focused our attention on anti-allergic drugs commonly prescribed for oral administration. Common side effects of anti-allergic oral medications are drowsiness, headache, trouble sleeping etc;[48,49] we considered that these side effects could be overcome by converting the drug molecule into gel based self-delivery systems for topical applications. Cetirizine is a well known anti-allergic drug that has free carboxylic acid functionality (necessary for salt formation). Therefore, we planned to convert this monocarboxylic acid drug-cetirizine into simple organic salt based supramolecular topical gel for self-delivery applications.

For this purpose, we have chosen to react cetirizine with a series of primary amines namely, benzyl amine, phenethyl amine, tyramine, tryptamine, 1-methyl naphthyl amine and tris (2-aminoethyl) amine to form a new class of PAM salts (**1-6**) as plausible potential supramolecular gelators (Scheme 1). Among these salts, cetirizine-tyramine salt **3** displayed excellent ability to gel methylsalicylate which is commonly present in many commercially available topical gels/sprays/ointments etc. The gelator salt was also capable of forming methylsalicylate gel in presence of 1 % menthol producing a methylsalicylate/menthol topical gel. The biocompatibility of the gelator salt was evaluated by MTT assay in mouse

macrophage RAW 264.7 cell line and mouse myoblast C2C12 cell line. The methylsalicylate/menthol topical gel produced from the gelator salt **3** showed excellent *in vivo* self-delivery application in treating DNCB–induced allergic ear redness and skin contact hypersensitivity in mice. Thus, simple salt formation rationale was effective in designing anti-allergic drug based supramolecular topical gel that has successfully been used to treat DNCB induced skin contact hypersensitivity in mice following self-delivery approach.

2. Experimental Section

Materials: All the chemicals including cetirizine dihydrochloride, benzyl amine, phenethyl amine, tyramine, tryptamine, 1-methyl naphthyl amine and tris (2-aminoethyl) amine, menthol etc. were purchased from Sigma-Aldrich and used without further purification. Solvents were of analytical reagent (AR) grade and used without further distillation. Hair removing cream veet (Veet, India) and skin allergy inducing agent, 2, 4 – di nitro chlorobenzene (DNCB) (Avra, India) used in the *in vivo* experiments were purchased from the local market. Anti-mouse IL-5 and anti-mouse IFN-γ used in immunohistochemistry analyses were purchased from eBioscience. Immunohistochemistry staining was performed using mouse specific HRP/DAB (ABC) detection IHC kit (ab64259, Abcam Biotech Company).

General Methods: FT-IR spectra of the salts were recorded using Shimadzu FT-IR 8300 instrument. The elemental analyses were carried out using a Perkin-Elmer Precisely, Series-II, CHNO/S Analyser-2400. NMR spectra were recorded using 500 MHz NMR spectrometer (Bruker Ultrasheild Plus-500). HR-TEM images were taken using a JEOL instrument with 300 mesh copper TEM grid. Rheology studies were carried out using Anton Paar Modular Compact Rheometer (MCR 102). Methyl thiazolyldiphenyl tetrazolium bromide (MTT) assay was conducted using a multiplate ELISA reader (Varioskan Flash Elisa Reader, Thermo

Fisher). Dorsal skin photographs of the mice were taken using SONY Cyber-shot 16.2 megapixels camera. UV-Visible spectra of cetirizine and its salt were recorded using CARY BIO 100 UV-Visible spectrophotometer. Histology images were recorded using a LEICA MZ 16 microscope.

Synthesis of Salts:

Cetirizine dihydrochloride salt (5 mM, 2.3 g) was dissolved in 25 mL water and then an aqueous solution of $NaHCO_3$ (25 mL, 10 Mm, 0.84 g) was added to it and the mixture was taken in a separating funnel. HCl free cetirizine was extracted in dichloromethane from this mixture. Similarly, HCl free tyramine was prepared from the tyramine hydrochloride salt. All the salts (**1-6**) were synthesized by mixing HCl free cetirizine and the primary amines (benzyl amine, phenethyl amine, tyramine, tryptamine, 1-methyl naphthyl amine and tris (2-aminoethyl) amine) in 1:1 molar ratio in methanol at room temperature. The reaction mixture was sonicated for a few minutes for homogeneous mixing followed by evaporation of the solvent in a rotary evaporator. The resultant solid was isolated as the salt in near-quantitative yield.

Physico-chemical Data

Salt 1: Elemental analysis calculated for $C_{28}H_{34}ClN_3O_3 + 2H_2O$ (%): C, 63.21; H, 7.20; N, 7.90; found: C, 62.59; H, 6.92; N, 7.42. FT-IR (KBr Pellet): 1593 cm^{-1} (s, salt C=O stretch). ^1H NMR (500 MHz, MeOD, 25°C): δ = 7.37-7.16 (m, 14H), 4.18 (s, 1H), 3.92 (s, 2H) 3.86 (s, 2H), 3.56 (t, *J* = 8.0 Hz, 2H), 2.59-2.54 (d, *J* = 8.0 Hz, 6H), 2.31 (s, 4H) ppm. ^{13}C NMR (500 MHz, MeOD, 25°C): δ = 178.06, 143.23, 142.73, 138.77, 133.70, 130.46, 129.87, 129.71, 129.64, 129.24, 129.09, 128.93, 128.37, 76.39, 71.80, 67.68, 58.38, 54.13, 52.00, 49.24, 45.21 ppm (Figure S1).

Salt 2: Elemental analysis calculated for $C_{29}H_{36}ClN_3O_3$ (%): C, 68.29; H, 7.11; N, 8.24; found: C, 67.89; H, 6.88; N, 7.86. FT-IR (KBr Pellet): 1587 cm^{-1} (s, salt C=O stretch). ^{1}H-NMR (500 MHz, MeOD, 25°C): δ = 7.41-7.39 (t, *J* =8.0 Hz, 4H), 7.31-7.22 (m, 9H), 7.18-7.15 (t, *J* = 7.0 Hz, 1H), 4.28 (s, 1H), 3.87 (s, 2H), 3.63 (s, 2H), 3.07-3.04 (t, *J* = 8.0 Hz, 2H), 2.91-2.88 (d, *J* = 8.0 Hz, 2H), 2.74 (s, 6H), 2.45 (s, 4H) ppm. ^{13}C-NMR (500 MHz, MeOD, 25°C): δ = 178.20, 143.12, 142.60, 138.83, 133.79, 130.49, 129.86, 129.81, 129.75, 129.68, 128.96, 128.44, 127.98, 76.29, 71.65, 67.62, 58.31, 54.19, 51.74, 42.35, 35.94 ppm (Figure S2).

Salt 3: Elemental analysis calculated for $C_{29}H_{36}ClN_3O_4$ (%): C, 66.21; H, 6.90; N, 7.99; found: C, 65.87; H, 6.55; N, 7.56. FT-IR (KBr Pellet): 3377 cm^{-1} (brs, O-H stretch), 1581 cm^{-1} (s, salt C=O stretch). ^{1}H-NMR (500 MHz, MeOD, 25°C): δ = 7.43-7.41 (d, *J* =9.0 Hz,3H), 7.39 (s, 1H), 7.29-7.26 (dd, *J* = 5.0, 6.0 Hz, 4H), 7.20-7.17 (t, *J* = 7.5 Hz, 1H), 7.05-7.04 (d, *J* = 8.0 Hz, 2H), 6.74-6.72 (d, *J* = 8.5 Hz, 2H), 4.32 (s, 1H), 3.86 (s, 2H), 3.69-3.67 (t, *J* = 5.5 Hz, 2H), 2.99-2.96 (t, *J* = 8.0 Hz, 2H), 2.87-2.86 (d, *J* = 5.0 Hz, 6H), 2.78-2.75 (t, *J* = 7.5 Hz, 2H), 2.52 (s, 4H) ppm. ^{13}C-NMR (500 MHz, MeOD, 25°C): δ = 177.06, 156.24, 141.91, 141.38, 132.59, 129.54, 129.25, 128.51, 128.45, 128.26, 127.71, 127.20, 115.36, 75.02, 70.29, 66.40, 57.00, 52.99, 50.30, 41.61, 34.30 ppm (Figure S3).

Salt 4: Elemental analysis calculated for $C_{31}H_{37}ClN_4O_3$ +H_2O (%): C, 65.65; H, 6.93; N, 9.88; found: C, 66.15; H, 7.42; N, 9.42. FT-IR (KBr Pellet: 1585 cm^{-1} (s, salt C=O stretch). ^{1}H-NMR (500 MHz, MeOD, 25°C): δ = 7.55-7.53 (t, *J* =8.0 Hz,1H), 7.35-7.30 (m, 6H), 7.24-7.20 (t, *J* = 7.0, Hz, 5H), 7.15-7.10 (t, *J* = 7.0, Hz, 4H), 7.08-76.99 (t, *J* = 7.0, Hz, 1H), 4.13 (s, 1H), 3.86 (s, 2H) 3.54 (s, 2H), 3.12-3.06 (t, *J* = 8.0 Hz, 4H), 2.55-2.50 (M, *J* = 8.0 Hz, 8H), 2.29 (s, 4H) ppm. ^{13}C-NMR (500 MHz, MeOD, 25°C): δ = 178.12, 143.12, 142.61, 138.28, 133.68, 130.46, 129.66, 129.60, 128.94, 128.34, 124.25, 122.70, 119.99, 119.07, 112.57, 111.09, 76.30, 71.77, 67.68, 58.38, 54.12, 51.96, 41.31, 25.42 ppm (Figure S4).

Salt 5: Elemental analysis calculated for $C_{32}H_{36}ClN_3O_3 + 2H_2O$ (%): C, 66.02; H, 6.93; N, 7.22; found: C, 66.27; H, 6.54; N, 7.05. FT-IR (KBr Pellet): 1584 cm^{-1} (s, salt C=O stretch). ^{1}H-NMR (500 MHz, MeOD, 25°C): δ = 8.10-8.07 (d, *J* =8.4 Hz,1H), 7.92-7.90 (d, *J* =8.0 Hz,1H), 7.87-7.85 (d, *J* =8.0 Hz,1H), 7.61-7.46 (m, 4H), 7.40-7.36 (t, *J* =8.4 Hz, 4H), 7.27-7.25 (t, *J* = 6.4 Hz, 4H), 7.20-7.16 (t, *J* = 7.2 Hz, 1H), 4.43 (s, 1H), 4.24 (s, 2H), 3.88 (s, 2H), 3.70-3.67 (t, *J* = 5.5 Hz, 2H), 2.89 (m, 6H), 2.46 (m, 4H) ppm. ^{13}C-NMR (500 MHz, MeOD, 25°C): δ = 168.54, 141.75, 141.20, 140.54, 139.33, 138.94, 134.15, 132.66, 129.19, 128.73, 128.54, 128.48, 127.65, 127.26, 126.54, 125.93, 125.89, 125.33, 122.68, 74.78, 70.24, 65.82, 56.82, 52.75, 49.76, 41.30 ppm (Figure S5).

Salt 6: Elemental analysis calculated for $C_{25}H_{36}ClN_3O_6 + 3H_2O$ (%): C, 53.23; H, 7.51; N, 7.45; found: C, 52.67; H, 7.63; N, 7.57. FT-IR (KBr Pellet): 1608 cm^{-1} (s, salt C=O stretch), 3205 cm^{-1} (brs, O-H stretch). ^{1}H-NMR (500 MHz, MeOD, 25°C): δ = 7.43-7.39 (t, *J* =8.0 Hz,4H), 7.29-7.25 (m, 4H), 7.19-7.16 (t, *J* = 7.0, Hz, 1H), 4.31 (s, 1H), 3.87 (s, 2H) 3.68 (s, 2H), 3.55 (t, *J* = 8.0 Hz, 6H), 2.85 (d, *J* = 8.0 Hz, 6H), 2.52 (s, 4H), ppm. ^{13}C-NMR (500 MHz, MeOD, 25°C): δ = 171.26, 143.17, 142.62, 138.84, 130.49, 129.77, 129.70, 128.94, 128.45, 76.25, 71.50, 67.72, 63.46, 59.83, 58.17, 54.27, 51.45 ppm (Figure S6).

Gelation Experiment: In a typical gelation experiment, 20 mg of a salt was taken in a test tube (length = 100 mm and diameter = 15 mm) and dissolved in 0.5 mL of the targeted solvent by heating until a clear hot solution was formed. The clear solution was then allowed to cool to room temperature to form stable gel within a few minutes. Gel formation was confirmed by test tube inversion method.

T_{gel} Experiment: The gel-sol dissociation temperatures (T_{gel}) of all the gels of **3** were measured by the dropping ball method at various gelator concentrations. In this experiment, a glass ball of weighing 216.45 mg was placed on a 0.5 mL gel of various gelator concentration

starting from the MGC value, taken in a test tube (length = 100 mm and diameter = 15 mm). The test tube was then immersed in an oil bath placed on a magnetic stirrer to ensure uniform heating. The temperature was noted when the ball touched the bottom of the test tube.

Tranmission Electron Microscopy (TEM) Sample Preparation: Gel was painted on a carbon-coated Cu (300 mesh) TEM grid for each sample**.** The grid was dried under vacuum at room temperature for one day and used for recording TEM images using an accelerating voltage of 200 kV without staining.

Rheology Studies: The rheological response of of all the gels of **3** was studied under dynamic and steady shear measurement. All experiments were done at room temperature (25 °C) on parallel-plate geometry (25 mm diameter, 1 mm gap). Rheological experiments were carried out using Anton Paar Modular Compact Rheometer (MCR 102).

Single Crystal X-ray Diffraction: X-ray quality single crystals of the salt **5** and **6** were grown at room temperature via slow evaporation from methanol solvent. While salt **5** crystallized in the centrosymmetric monoclinic space group '*I*2/a' (nonstandard space group under *C*2/c), salt **6** crystallized in the centrosymmetric triclinic space group '*P*-1'. Data were collected using MoK_{α} (λ = 0.7107 Å) radiation on a BRUKER APEX II diffractometer equipped with CCD area detector. Data collection, data reduction, structure solution/refinement were carried out using the software package of SMART APEX-II. All structures were solved by direct method. Nonhydrogen atoms were treated anisotropically. All the hydrogen atoms were geometrically fixed. CCDC number 1053907 and 1053908 for salt **5** and **6** respectively contain the supplementary crystallographic data for this paper. These data can be obtained free of charge via www.ccdc.cam.ac.uk/conts/retrieving.html (or from the Cambridge Crystallographic Data Centre, 12 Union Road, Cambridge CB21EZ, UK; fax: (+44) 1223-336-033; or deposit@ccdc.cam.ac.uk).

MTT Assay: The mouse macrophage RAW 264.7 cells and mouse myoblast C2C12 cells were purchased from American Type Culture Collection (ATCC) and maintained following their guidelines. The cells were grown in Dulbecco's Modified Eagle's Medium (DMEM) medium supplemented with 10% fetal bovine serum (FBS) and 1% penicillin and streptomycin in a humidified incubator at 37 °C and 5% CO_2. Approximately 1×10^4 cells/well were seeded in 96-well plates. After 24 h of seeding, the cells were treated with various concentrations (up to 400 μM) of cetirizine, the salt **3** or DMEM alone for 72 h in a humidified incubator at 37 °C and 5% CO_2. Then, the culture medium was replaced with 100 μg of MTT per well and kept at 37 °C for 3 h. DMSO (100 μL/well) was added to dissolve the formazan produced by mitochondrial reductase from live cells and the plate was further incubated for 30 minutes at 37 °C. The absorbance of formazan was recorded at 570 nm using a multiplate ELISA reader (Varioskan Flash Elisa Reader, Thermo Fisher). The percentage of live cells in cetirizine and the salt-treated sample was calculated by considering the DMEM-treated sample as 100%.

Preparation of Methylsalicylate/Menthol Topical Gel 3: 30 mg salt **3** (3 % w/v) and 10 mg menthol (1 % w/v) were dissolved in 1.0 mL methylsalicylate by heating and the hot clear solution was then allowed to cool to room temperature. After few minutes opaque gel formation was observed.

Animals Experiment: All the BALB/c male mice of aged 10-12 weeks were maintained in the animal house facility of Department of Biological Chemistry, Indian Association for the Cultivation of Science, Kolkata as per guidelines of Institutional Animal Ethics Committee (IAEC). All animal experiments were approved by a local animal ethics committee (Institutional Animal Ethical Committee (IAEC), Indian Association for the Cultivation of Science, Kolkata-700032, India; Chairman/Member Secretary of Institutional Animal Ethical Committee (IAEC): Dr. Susanta Roychoudhury). The animals were housed in separate cages

under controlled conditions of temperature at 24 ± 2°C with 12 h-12 h light-dark cycle in experimental period. The animals were allowed free access to food and water throughout the experiment.

Histology Experiment: After twelve days treatment, dorsal skin tissue samples were collected from one mouse of each group. The skin tissues were fixed in 10% formalin and embedded in paraffin wax and each section was stained with hematoxylin-eosin (H & E) and toluidine blue and examined by LEICA MZ 16 optical microscope.

Immunohistochemistry (IHC) Experiment: Immunohistochemistry staining was performed according to the manufacturer's protocol (Mouse specific HRP/DAB (ABC) Detection IHC Kit (ab64259), Abcam Biotech Company). In brief, the poly-l-lysine coated slides containing paraffin-embedded tissue sections were first deparaffinised with xylene and rehydrated with ethanol/water. The endogenous peroxidase and biotin activities in the tissue sections were then blocked by treating with H_2O_2 and bovine serum albumin (BSA), respectively and the slides were incubated overnight at 4º C in a humidified chamber with a primary antibody (anti- mouse IFN-γ, eBioscience product number BMS182 or anti-mouse IL-5, eBioscience product number 14-7052). The tissue sections were then treated with the biotinylated secondary antibody followed by treating with streptavidin peroxidase which was further stained with 3, 3-diaminobenzidine (DAB). Immunohistomounting media was added on the stained tissue sections before visualizing the slides under light microscope. Four mice per group were used, and a representative slide for each group is shown.

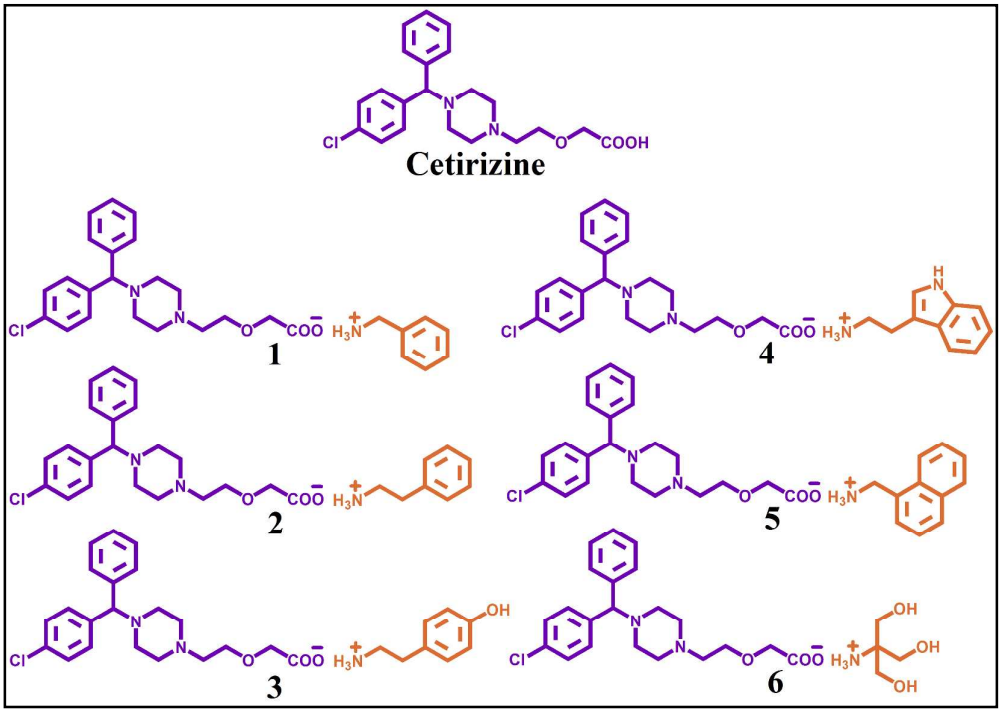

Scheme 1. Various salts **1-6** derived from anti-allergic drug cetirizine.

3. Results and Discussion

Synthesis

All the salts were prepared by reacting the monocarboxylic acid drug-cetirizine and the primary amines in 1:1 molar ratio in methanol. The reaction mixture was sonicated for a few minutes for homogenious mixing at room temperature followed by evaporation of the solvent in a rotary evaporator. The resultant solid was isolated as the salt in near-quantitative yield. Absence of $>C=O_{COOH}$ stretching band at 1741 cm^{-1} of cetrizine and presence of $>C=O_{COO}^-$ stretching band at 1587-1581 cm^{-1} of these salts confirmed complete proton transfer (salt formation) as revealed in the corresponding FT-IR spectra (Figure S7).

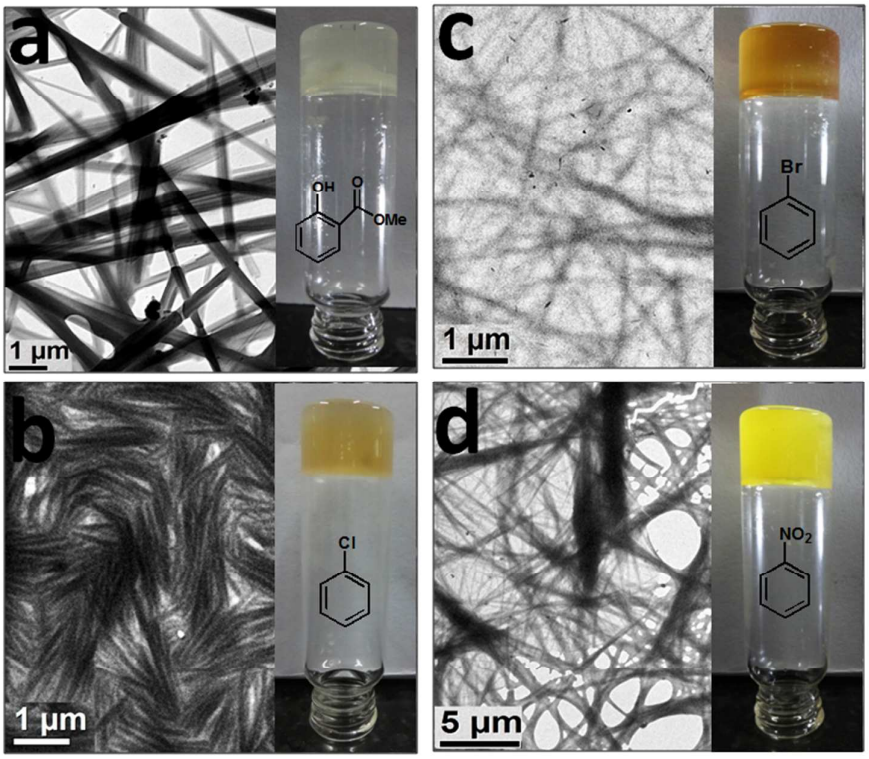

Figure 1. HR-TEM micrographs of (a) methylsalicylate, (b) chlorobenzene, (c) bromobenzene and (d) nitrobenzene gels of salt **3**. Insets are optical images of the corresponding gel.

Gelation and Characterization

We checked gelation ability of these salts **1-6** in various solvents. Among these salt **3** derived from cetirizine and tyramine was found to be capable of forming gel with methylsalicylate, chlorobenzene, bromobenzene and nitrobenzene. The minimum gelator concentrations (MGCs) of these gels were within 2.0 - 3.0 wt % and the corresponding gel-sol dissociation temperatures (T_{gel}) were within 106-108°C displaying the efficiency of the gelator as well the remarkable thermal stability of the gels (Table S1). Gel formation was confirmed by the test tube inversion method wherein the gel formed was found to be able to hold its weight against gravity when the container was placed upside down. Methylsalicylate and chlorobenzene gels of **3** were translucent whereas the corresponding bromobenzene and nitrobenzene gels were opaque (Figure 1). Table top rheology[50] (T_{gel} *vs* gelator concentration plot) revealed that

various supramolecular interactions were responsible for gel network formation as indicated by the steady increase of T_{gel} with the increase in gelator concentration (Figure S8).

The morphologies of methylsalicylate, chlorobenzene and nitrobenzene gels of **3** were found to be 1D tapes while that of bromobenzene gel was micro fibres. In all the cases, as anticipated, the tape/fibers were entangled to form the self-assembled network as observed under high resolution-transmission electron microscope (HR-TEM) (Figure 1) and within these networks solvents molecules were trapped resulting in gels.

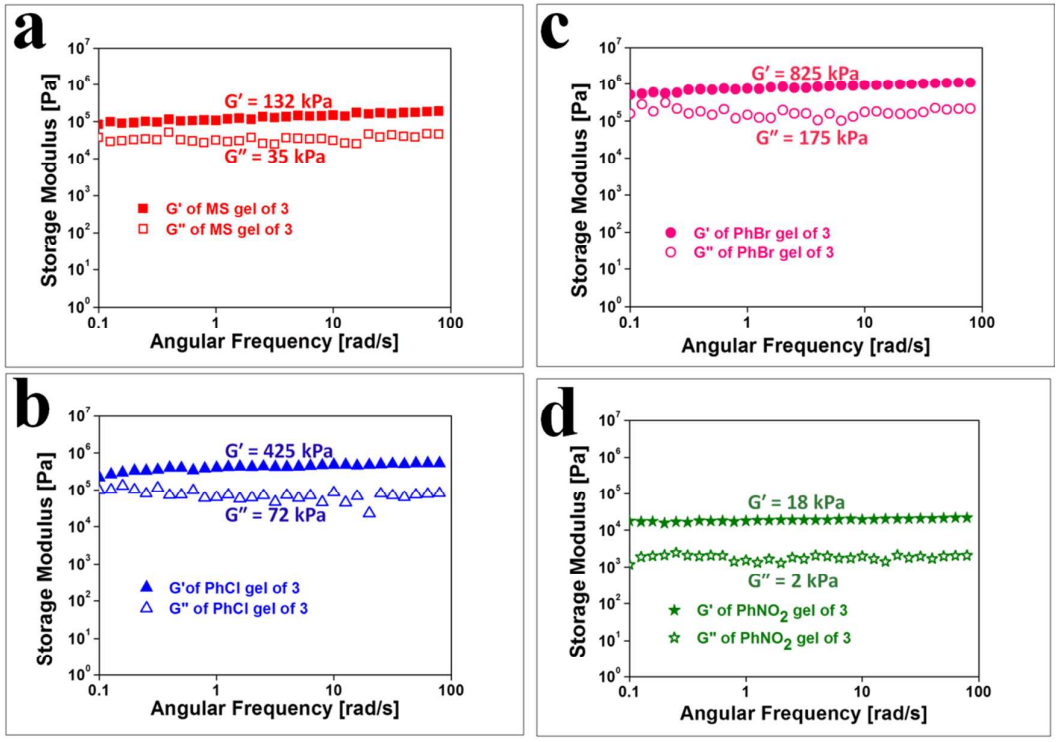

Figure 2. Frequency sweep rheological behaviour of (a) methylsalicylate (MS), (b) chlorobenzene (PhCl), (c) bromobenzene (PhBr) and (d) nitrobenzene ($PhNO_2$) gels of **3** at constant strain of 0.1 %.

In order to establish and assess the visco-elastic nature of these gels of **3**, we performed various rheological studies such as strain sweep and frequency sweep experiments. We first carried out strain sweep experiments for all the gels of **3** to find out the linear viscoelastic region that was needed to decide on the strain required to carry out frequency sweep

experiments. The strain sweeps were carried out in the strain range from 0.01 to 100% at a fixed frequency of 1 rad/s. Figure S9 showed the strain sweep behaviour of all the gels. The elastic modulus (G′) of these gels decreased rapidly and fell below the viscous modulus (G″) after the critical strain region (critical strain = 4, 10, 4 and 20 % for methylsalicylate (MS), chlorobenzene (PhCl), bromobenzene (PhBr) and nitrobenzene ($PhNO_2$) gel of **3,** respectively) indicating collapse of the gel network beyond the critical strain.

The frequency sweep plot displayed variation of G′ and G″ of these gels against the angular frequency ω under constant strain of 0.1 % as suggested by the independent strain sweep experiments. It was observed that G′ was higher than G″ in all the cases over the entire range of frequency ω, and they were largely frequency-invariant displaying the visco-elastic response typical of a gel. The value of G′ of all the gels clearly suggested that the bromobenzene gel was mechanically the strongest one (Figure 2).

Single Crystal X-ray Diffraction (SXRD)

In order to study the supramolecular synthon and its implication in gelation, we undertook SXRD studies of these salts. Despite our best efforts, we were able to generate X-ray quality single crystals of the non gelator salts **5** and **6** via slow evaporation of the methanol solution of the corresponding salts. The experimental data and hydrogen bonding parameters of these crystals are given in Table S2-4, Figure S10-11. Salt **5** crystallized in the centrosymmetric monoclinic space group '*I*2/a' (nonstandard space group under *C*2/c) with one ion pair and two solvate water molecules in the asymmetric unit. The ammonium cation was involved in hydrogen bonding interactions with the O atoms of carboxylate and pipyridine N of the drug molecule (anionic part) resulting in a discrete hydrogen bonded complex (Figure 3a) which further propagated into two dimensional via lattice occluded water mediated hydrogen bonding (Figure 3b).

Salt **6** crystallized in the centrosymmetric triclinic space group '*P*-1' with two ion pairs and five solvate water molecules in the asymmetric unit. The ammonium cation equipped with three –OH groups was found to be involved in various hydrogen bonding. The cationic part (-NH_3^+) was found to be involved in hydrogen bonding with the –OH group of neighbouring cationic moiety, carboxylate O and solvate water molecule (Figure 3c). The overall hydrogen bonding network in this salt was found to be two dimensional (Figure 3d). Thus, the typical 1D HBN was not observed in these nongelator salts presumably because of the additional hydrogen bonding functionalities (pipyridine N in drug moiety and –OH in amine) which helped in occluding guests molecules (water) in the crystal structures. However, such nongelling behaviour corroborated well with the structure-property correlation hypothesis of supramolecular gels.[42]

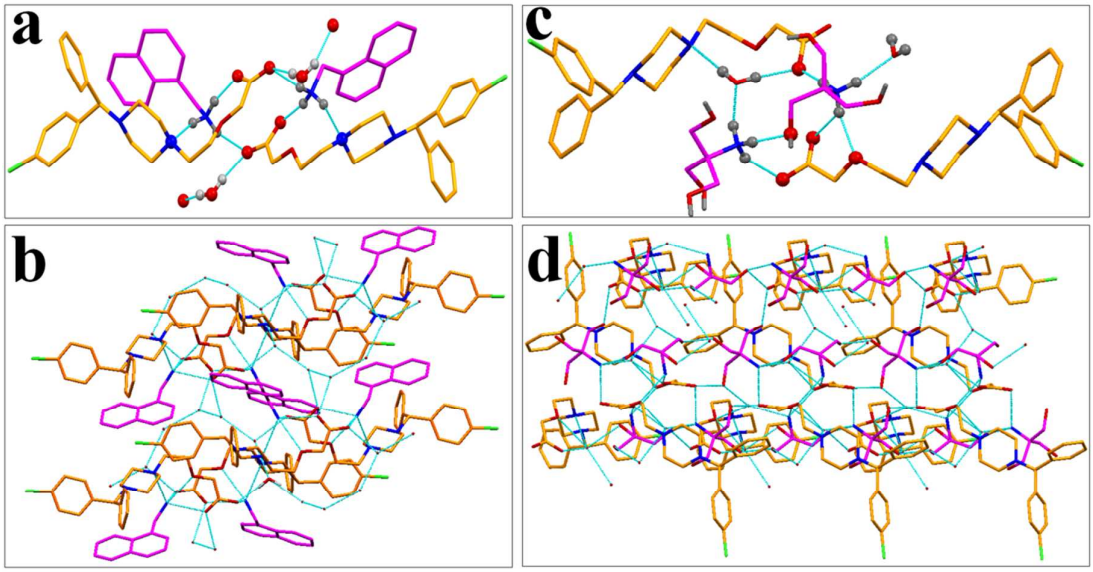

Figure 3. Crystal structure illustrations displaying various hydrogen bonding involving the ion pair and the solvate water in (a) salt **5**, (c) salt **6**; solvate water mediated 2D hydrogen bonded network in (b) salt **5**, (d) salt **6**.

FT-IR Studies of Salt 3

We performed detailed FT-IR studies of salt **3**. Since the >C=O stretching band of methylsalicylate (~1680 cm^{-1}) and N=O stretching band of nitrobenzene (~1550 cm^{-1}) overlap with the stretching frequency of COO^- group (1650-1550 cm^{-1}), we decided to carry out FT-

IR experiments of salt **3** using the solvents chlorobenzene and bromobenzene as these solvents do not have any overlapping band with that of COO^- group. The results revealed that the COO^- stretching band of solid salt **3** (1582 cm^{-1}) was red-shifted (~1574 cm^{-1}) in chlorobenzene and bromobenzene gels indicating slightly stronger hydrogen bonding interactions in the gel state compared that in the bulk solid. However, the stretching bands of the xerogels shifted towards the values observed in the bulk solid (1582 and 1576 cm^{-1} for chlorobenzene and bromobenzene xerogels, respectively) which clearly indicated that the gelling solvents played a crucial role in the self-assembly process (Figure S12).

Biological Studies

Having successfully converted one of the cetirizine salts (salt **3**) into a supramolecular gelator, we undertook various biological studies in order to develop a topical gel formulation for self-application.

***In vitro* studies**

Physiological stability

We first evaluated stability of the gelator salt **3** under physiological conditions using UV-Visible spectroscopy. For this purpose, the gelator salt **3** was incubated in PBS of pH 7.4 at 37 °C and 5 % CO_2 atmosphere in a humidified incubator for 24 and 72 h. The UV-Visible spectra of both 24 and 72 h incubated samples appeared to be identical with that of the gelator salt **3** in PBS at room temperature. These spectra differed from that of the parent drug cetirizine by an absorption band at 274 nm which was attributed to the bezenoid band of the phenolic moiety of tyramine cation indicating that no chemical degradation of the individual component of salt **3** in PBS after incubation (Figure S13).

Biocompatibility

Next, we checked the cell viability test of the gelator salt **3** in order to evaluate its potential application in self-delivery. For this purpose, RAW 264.7 macrophage cells were treated with

various concentrations of both cetirizine and salt **3** for 72 h at 37 °C, and cell viability test was performed using MTT assay.[51] Figure 4a showed that ~ 40% RAW 264.7 cells survived after 72 h incubation at salt concentration of 400 µM for both cetirizine and the gelator salt **3**. These results indicated that the biocompatibility of the gelator salt **3** was comparable to that of its parent drug cetirizine. We also checked the cell viability of the gelator salt **3** in mouse myoblast C2C12 cell line wherein the cell viability results of salt **3** was comparable to that obtained from macrophage RAW 264.7 cell line (Figure 4b).

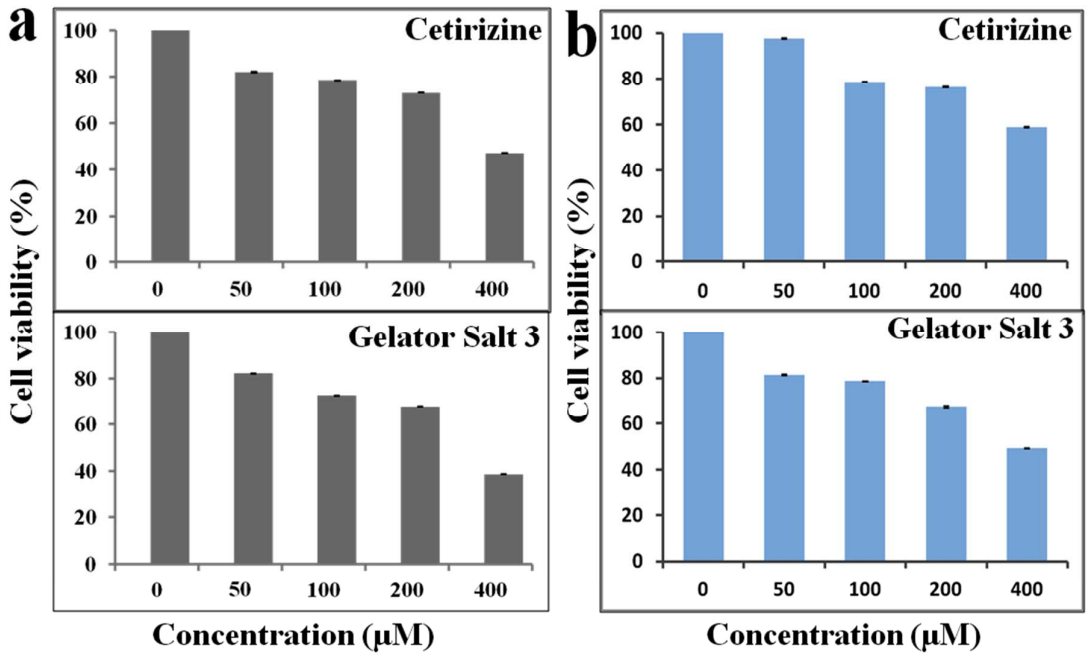

Figure 4. MTT assay of both cetirizine and the gelator salt **3**; (a) MTT assay in mouse macrophage RAW 264.7 cell line for 72 h at 37 °C; (b) MTT assay in mouse myoblast C2C12 cell line for 72 h at 37 °C.

In vivo studies

Self-delivery of topical gel 3 in treating skin allergic inflammation in mice

Encouraged by the physiological stability and biocompatibility of the gelator salt **3**, we decided to evaluate its possibility of self-delivery as a topical gel in treating DNCB induced skin allergic-inflammation in mice. Contact hypersensitivity of skin (swelling/redness) in

mice induced by DNCB has been commonly used animal model for studying the effect of potential anti-allergic drug.[52] For this purpose, we have followed a published literature protocol.[53] DNCB induced contact hypersensitivity of ears is well known[52] and used as preliminary lead in such studies. BALB/c male mice (n=10, 1 mouse/cage) of aged 10-12 weeks were divided into two groups – Group A (2 mice) and Group B (8 mice). The left ear of Group A mice were painted with 20 µL ethanol while that of the mice of group B were painted with 20 µL 2% DNCB solution in ethanol. The same sensitization was repeated after 30 minutes. All the DNCB treated mice (group B) showed marked allergic redness on the left ears as compare to the right ears. No such redness was observed in the control group mice (group A). Group B mice were then divided into four sub groups (2 mice in each group) namely B1, B2, B3 and B4. No treatment was applied in B1 mice. The mice in B2 were treated by painting 20 µL 2 % menthol in methylsalicylate. The treatment provided to the mice in group B3 was by the application of 20 µL mixture of 2 % menthol and 2 % cetirizine in methylsalicylate. Finally, group B4 mice were trated with 20 µL mixture of 2 % menthol and 2 % gelator salt **3** in methylsalicylate. One hour post treatment, the left ears of group B4 mice showed marked improvement displaying significantly less allergic redness as compare to the non-treated mice in B1 and B2. It may be noted that the improvement in ear redness in group B3 mice (cetirizine treated) was comparable to that in group B4 mice (gelator salt **3** treated) indicating that the gelator salt **3** derived topical gel could be applied in treating DNCB induced skin contact hypersensitivity in mice (Figure 5).

Thus, a 3 wt % methylsalicylate/menthol topical gel of salt **3** was employed to study its effect on the DNCB induced allergic skin contact hypersensitivity in mice. Menthol was used in the topical gel formulation because of its vasodilation effects (skin softening) allowing easy penetration of the active ingredient (drug) through the skin barrier. In these experiments, the dorsal skin hair of BALB/c male mice (n=20, aged 10-12 weeks, 1 mouse/cage) were

removed by applying hair removing cream veet and the mice were rested for two days. The mice were then divided into two groups – group X (4 mice) and Y (16 mice). Mice in group X and Y were first sensitised with 100 µL ethanol and 100 µL 2% DNCB solution in ethanol, respectively. The same sensitization was repeated after 7 days in both the groups. After 3 days of the last sensitization, allergy like (swelling, erythema, edema, excoriation etc.) symptoms were observed on the dorsal skin of all the DNCB-induced mice (group Y) while ethanol treated group X mice showed normal skin coloration. Group Y mice were further divided into four sub groups (4 mice in each group) – Y1, Y2, Y3 and Y4. The mice in Y1 were not treated whereas Y2, Y3 and Y4 were treated with 1% menthol containing methylsalicylate (50µL/day), 1% menthol containing cetrizine solution in methylsalicylate (50µL/day delivering 1 mg of cetrizine) and 1% menthol containing methylsalicylate/menthol topical gel of salt **3** (40 mg/day delivering 1 mg of gelator salt **3**), respectively. The above said treatment was continued daily for 6 more days.

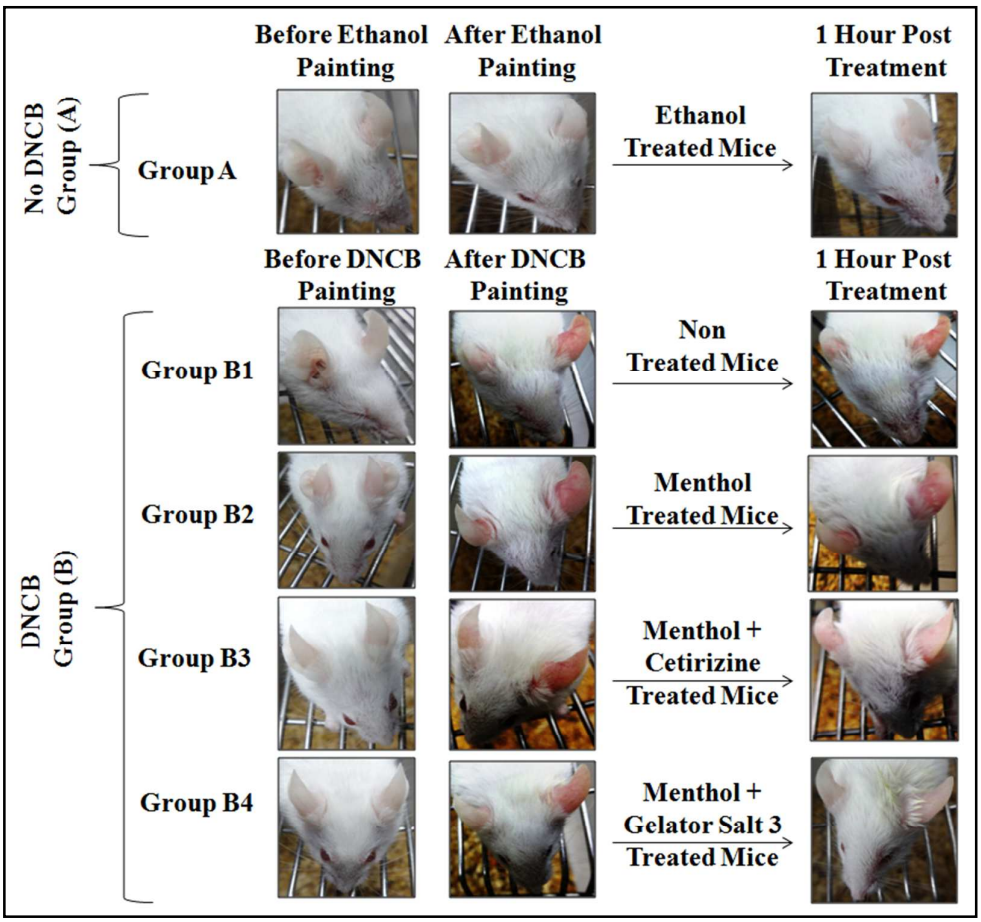

Figure 5. DNCB-induced allergic ear redness observation in the right ears of BALB/c male mice after various treatments. (Group A) no skin allergic induction by DNCB as the normal mice; (Group B1) no treatment after skin allergy induction by DNCB; (Group B2) solution of menthol application after skin allergy induction by DNCB; (Group B3) solution of mother drug cetirizine application after skin allergy induction by DNCB; and (Group B4) solution of gelator salt **3** application after skin allergic induction by DNCB.

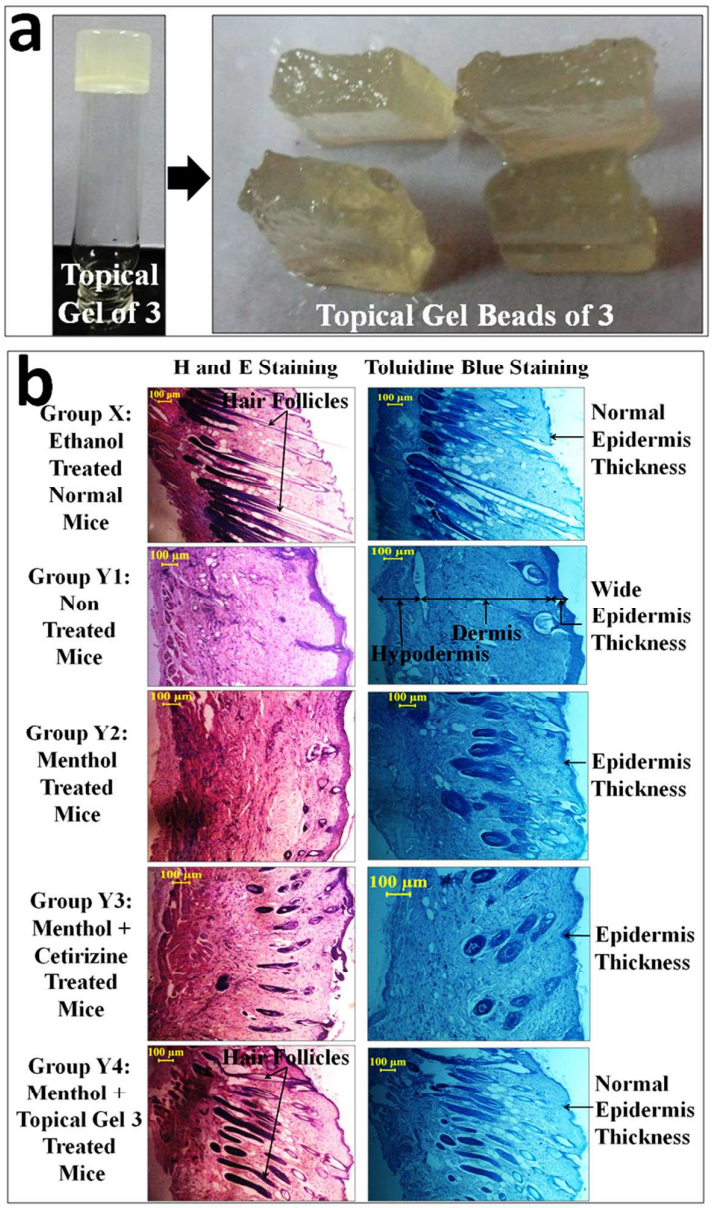

Figure 6. (a) Methylsalicylate/menthol topical gel and gel beads of salt **3**; (b) Histological features of the dorsal skin tissues of mice. (Group X) no skin allergic induction by DNCB as the normal mice; (Group Y1) no treatment after skin allergy induction by DNCB; (Group Y2) menthol solution application after skin allergy induction by DNCB; (Group Y3) mother drug cetirizine solution application after skin allergy induction by DNCB; and (Group Y4)

methylsalicylate/menthol topical gel of salt **3** application after skin allergic induction by DNCB.

Histology

To see the effects of treatment on the dorsal skin of these various group of mice described in the previous section, we performed histology. For this purpose, we collected the dorsal skin tissues of the various groups after 12 days treatment and subsequently, the cross sections of the skin tissues were fixed in 10% formalin and embedded in paraffin wax; each section was stained with hematoxylin-eosin (H & E). The H & E stained tissue images revealed that the hair follicles[54] were present in the group X normal mice whereas no hair folicles were observed in the non treated group Y1 mice. In group Y2 (menthol treated) and Y3 (cetrizine treated) mice, a few growing hair folicles were observed whereas the topical gel **3** treated group Y4 mice showed a number of well grown hair folicles, which were similar to that of the group X normal mice. We also examined epidermis thickness[55] of the dorsal skin of the mice under various treatment groups after staining their dorsal skin tissues with toluidine blue. The average epidermal thickness of the dorsal skin was 9.9 ± 1.5 μm in the normal group mice (X), 48.5 ± 8.6 μm in the non treated group mice (Y1), 22.4 ± 2.1 μm in the menthol treated group mice (Y2), 15.2 ± 3.3 μm in the cetirizine treated group mice (Y3), and 9.8 ± 1.2 μm in the topical gel **3** treated group mice (Y4). These results showed that the epidermis thickness of the topical gel **3** treated mice (group Y4) was comparable to that of the normal mice (group X) (Figure 6). These data clearly indicated that the topical gel **3** was effective in treating the allergic skin conditions. Thus, it was possible to self deliver salt **3** in the form of a

supramolecular topical gel in treating DNCB induced allergic skin contact hypersensitivity in mice.

Immunohistochemistry (IHC)

Finally, we carried out immunohistochemistry staining of the dorsal skin tissues of mice to see the effects of the various treatments on T cells (Th1/Th2)-derived cytokines, since allergic inflammation is associated with the balance between Th1 and Th2 cells. Under allergic condition Th1 cells derived cytokine such as interferon gamma (IFN-γ) down-regulate and Th2 cells derived cytokine such as interleukin 5 (IL-5) up-regulate.[56] Immunohistochemistry staining was performed according to the manufacturer's protocol using mouse specific HRP/DAB (ABC) detection IHC kit (ab64259, Abcam Biotech Company). In these experiments, the slides containing paraffin-embedded tissue sections were first deparaffinised with xylene and rehydrated with ethanol/water. The endogenous peroxidase and biotin activities in the tissue sections were then blocked by treating with H_2O_2 and bovine serum albumin (BSA), respectively and the slides were incubated overnight at 4º C in a humidified chamber with a primary antibody (1:300 dilution of the stock anti- mouse IFN-γ or anti-mouse IL-5 anti-body in PBS). The tissue sections were then treated with the biotinylated secondary antibody followed by treating with streptavidin peroxidase which was further treated with 3, 3-diaminobenzidine (DAB) to produce DAB-brown-an easily observable brown coloured oxized product of DAB. Thus, by the intensity of borwn color, the up or down regulation of the cytokines (IFN-γ or IL-5) could be monitored. Immunohistochemical analyses revealed that ethanol treated normal mouse (group X) had more IFN-γ (as high Th1 cytokines present in normal condition) and less IL-5 (as low Th2 cytokine present in normal condition) positive cells while DNCB-painted non treated allergic mice (group Y1) showed less IFN-γ (as Th1 cytokine down-regulate in allergy) and more IL-5 (as Th2 cytokine up-regulate in allergy) positive cells as expected. However, treatment with

menthol solution (group Y2) led to a marked increase in IFN-γ positive cells with a decrease in IL-5-positive cells with respect to that of the non treated mice indicating the partial recovery of the allergic condition. Again, treatment with cetirizine (group Y3) or the topical gel **3** (group Y4) displayed further improvement of allergic conditions as revealed by the marked upregulation of IFN-γ and down regulation of IL-5 comparted to that of in gropu Y1 (menthol treated). However, the appearence of more hair follicles in group Y4 as compared to that of in the group Y3 clearly indicated the effectiveness of the topical gel **3** in treating the allegy induced skin condition in mice (Figure 7).

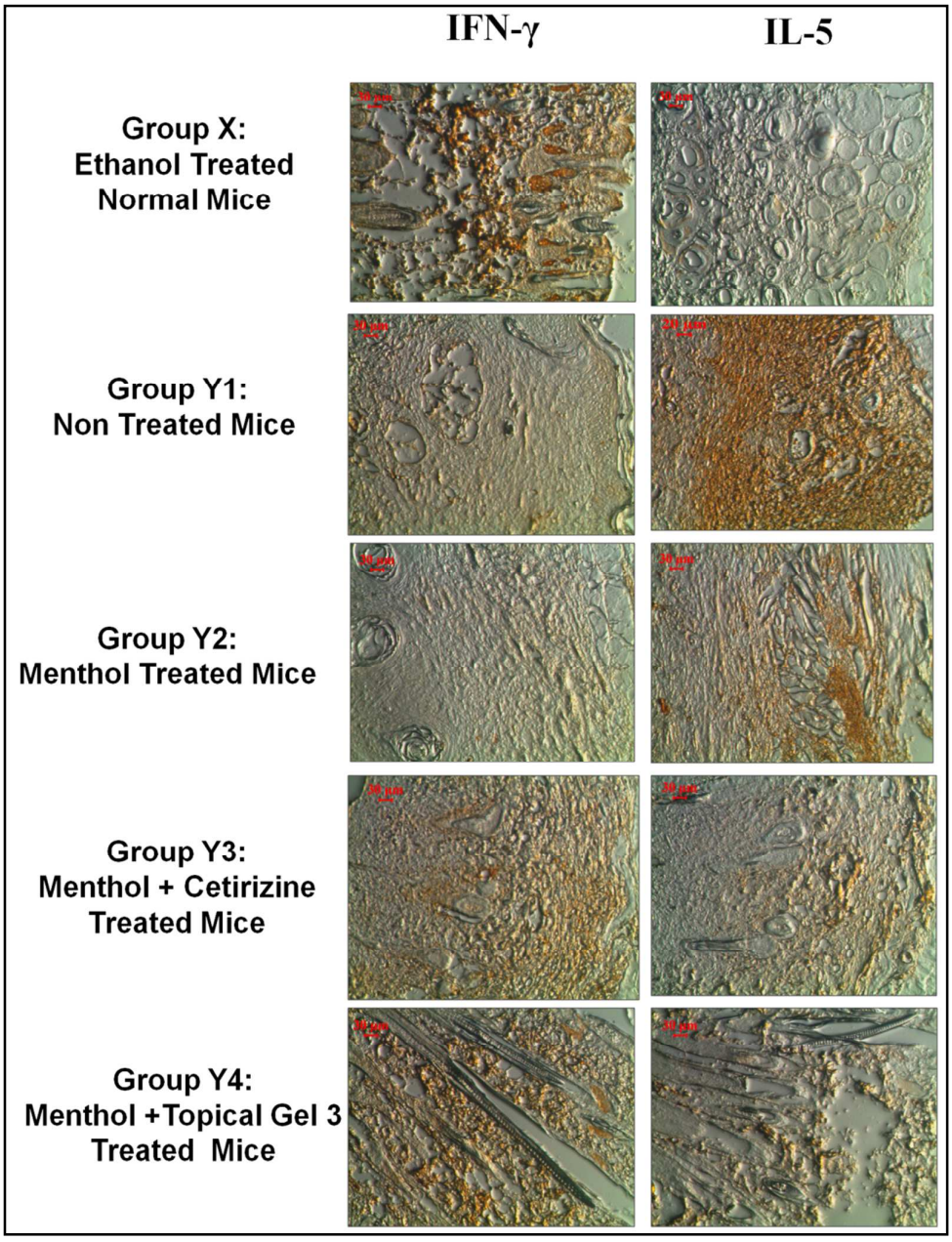

Figure 7. Comparison of IFN-γ and IL-5 immunohistochemical staining of the dorsal skin tissues of mice. (Group X) no skin allergic induction by DNCB as the normal mice; (Group Y1) no treatment after skin allergy induction by DNCB; (Group Y2) menthol solution application after skin allergy induction by DNCB; (Group Y3) mother drug cetirizine solution application after skin allergy induction by DNCB; and (Group Y4) methylsalicylate/menthol topical gel of salt **3** application after skin allergic induction by DNCB.

4. Conclusion

Herein we demonstrated that an anti-allergic drug namely cetrizine could easily be converted to a gelator (salt **3**) by following simple salt formation strategy based on supramolecular synthon rationale. Salt **3** displayed excellent capability of forming supramolecular topical gel with methylsalicylate/menthol. It was physiolgically stable and biocompatible in both mouse macrophage RAW 264.7 and mouse myoblast C2C12 cell line (MTT assay). *In vivo* experiments revealed that the topoical gel of salt **3** in methylsalicylate/menthol was able to treat DNCB–induced allergic ear redness and skin contact hypersensitivity in BALB/c mice. The fact that the topical gel (salt **3**) application was indeed effective in treating the above mentioned allergic conditions was evident from the reduction of epidermis skin thikness and excellent growth of hair folicles as revealed in the histology studies. Immunohistochemistry assay further confirmed the Th1/Th2 cytokine-mediated pathway in such allergic conditions. The system developed herein is an excellent example of self-dellivery application of an anti-allergic drug wherein the requirement of additional gel matrix such as carbomer, hydroxypropyl cellulose, polysorbate, propylene glycol, glycerides etc. commonly used in commercial topical gel formulation is completely avoided. Moreover, covalent synthetic modification to convert a drug molecule into a supramolecular gelator is time-consuming and non-trivial whereas non-covalent (supramolecular) modification described herein (salt

formation) is time-economic and simple, and may be exploited in generating other drug based supramolecular gelators for various biomedical applications.

Acknowledgements

PD and SSJ thank Department of Bio-technology (DBT), New Delhi for financial support (DBT project number: BT/01/CEIB/11/V/13). J.M. thanks CSIR, New Delhi for senior research fellowship (CSIR grant number: 09/080(0776)/2011-EMR-1). JD and AH thank DBT and DST-New Delhi, respectively for Research Associateship. *In vitro* and *in vivo* biological experiments were carried out by JM. under the supervision of SSJ. Immunohistochemistry studies were carried out by JD. SXRD data were refined by AH.

Electronic Supplementary Information (ESI) available:

^{1}H-NMR, ^{13}C-NMR, FT-IR and UV-Visible spectra of the salts, T_{gel} vs gelator concentration plot, rheological plots, CCDC number 1053907 and 1053908 for crystal structures **5** and **6** and crystal parameters tables.

References

1. K. E. Uhrich, S. M. Cannizzaro, R. S. Langer and K. M. Shakesheff, *Chem. Rev.*, 1999, **99**, 3181.
2. G. Vilar, J. Tulla-Puche and F. Albericio, *Curr. Drug Delivery,* 2012, **9**, 367.

3. P. K. Vemula, J. Li and G. John, *J. Am. Chem. Soc.,* 2006, **128**, 8932.
4. M. J. Webber, J. B. Matson, V. K. Tamboli and S. I. Stupp, *Biomaterials,* 2012, **33**, 6823.
5. J. Li, Y. Kuang, Y. Gao, X. Du, J. Shi and B. Xu, *J. Am. Chem. Soc.,* 2013, **135**, 542.
6. J. Majumder, J. Deb, M. R. Das, S. S. Jana and P. Dastidar, *Chem. Commun.,* 2014, **50**, 1671.
7. R. Roy, J. Deb, S. S. Jana and P. Dastidar, *Chem. Eur. J.*, 2014, **20**, 15320.
8. P. Terech and R. G. Weiss, *Chem. Rev.,* 1997, **97**, 3133.
9. L. A. Estroff and A. D. Hamilton, *Chem. Rev.,* 2004, **104**, 1201.
10. M. Suzuki and K. Hanabusa, *Chem. Soc. Rev.,* 2009, **38**, 967.
11. C. Tomasini and N. Castellucci, *Chem. Soc. Rev.,* 2013, **42**, 156.
12. V. K. Praveen, C. Ranjith and N. Armaroli, *Angew. Chem. Int. Ed.,* 2014, **53**, 365.
13. Q. Lin, B. Sun, Q.-P. Yang, Y.-P. Fu, X. Zhu, Y.-M. Zhang and T.-B. Wei, *Chem. Commun.,* 2014, **50**, 10669.
14. M. George and R. G. Weiss, *Acc. Chem. Res*., 2006, **39**, 489.
15. A. R. Hirst, B. Escuder, J. F. Miravet and D. K. Smith, *Angew. Chem. Int. Ed.,* 2008, **47**, 8002.
16. M. Ikeda, K. Fukuda, T. Tanida, T. Yoshii and I. Hamachi, *Chem. Commun.,* 2012, **48**, 2716.
17. Q. Lin, T.-T. Lu, X. Zhu, B. Sun, Q.-P. Yang, T.-B. Wei and Y.-M. Zhang, *Chem. Commun.,* 2015, **51**, 1635.
18. A. Wynne, M. Whitefield, A. J. Dixon and S. Anderson, *J. Dermatol. Treat*., 2002, **13**, 61.
19. H. Basit, A. Pal, S. Sen and S. Bhattacharya, *Chem. Eur. J.,* 2008, **14**, 6534.
20. B. Escuder, F. Rodrguez-Llansola and J. F. Miravet, *New J. Chem*., 2010, **34**, 1044.

21. E. Carretti, M. Bonini, L. Dei, B. H. Berrie, L. V. Angelova, P. Baglioni and R. G. Weiss, *Acc. Chem. Res.,* 2010, **43**, 751.

22. K. Y. Lee and D. J. Mooney, *Chem. Rev.,* 2001**, 101,** 1869.

23. Z. A. C. Schnepp, R. Gonzalez-McQuire and S. Mann, *Adv. Mater.,* 2006**, 18**, 1869.

24. Z. Yang, G. Liang, M. Ma, A. S. Abbah, W. W. Lu and B. Xu, *Chem. Commun.,* 2007, 843.

25. S. Kiyonaka, K. Sada, I. Yoshimura, S. Shinkai, N. Kato and I. Hamachi, *Nat. Mater.,* 2004, **3**, 58.

26. K. J. C. van Bommel, M. C. A. Stuart, B. L. Feringa and J. van Esch, *Org. Biomol. Chem.,* 2005, **3**, 2917.

27. S. Bhuniya, Y. J. Seo and B. H. Kim, *Tetrahedron Lett.,* 2006, **47**, 7153.

28. X. M. Li, J. Y. Li, Y. A. Gao, Y. Kuang, J. F. Shi and B. Xu, *J. Am. Chem. Soc.,* 2010, **132**, 17707.

29. Q. Wang, Z. Yang, X. Zhang, X. Xiao, C. K. Chang and B. Xu, *Angew. Chem., Int. Ed.,* 2007, **46**, 4285.

30. S. M. Standley, D. J. Toft, H. Cheng, S. Soukasene, J. Chen, S. M. Raja, V. Band, H. Band, V. L. Cryns1 and S. I. Stupp, *Cancer Res*., 2010, **70**, 3020.

31. V. Jayawarna, M. Ali, T. A. Jowitt, A. F. Miller, A. Saiani, J. E. Gough and R. V. Ulijn, *Adv. Mater.,* 2006, **18**, 611.

32. K. Yoza, Y. Ono, K. Yoshihara, T. Akao, H. Shinmori, M. Takeuchi, S. Shinkai and D. N. Reinhoudt, *Chem. Commun.,* 1998*,* 907.

33. K. J. C. van Bommel, C. van der Pol, I. Muizebelt, A. Friggeri, A. Heeres, A. Meetsma, B. L. Feringa and J. van Esch, *Angew. Chem. Int. Ed.,* 2004*,* **43**, 1663.

34. O. Lebel, M. E. Perron, T. Maris, S. F. Zalzal, A. Nanci and J. W. Wuest, *Chem. Matter.,* 2006, **18**, 3616.

35. M. Suzuki, H. Saito and K. Hanabusa, *Langmuir*, 2009, **25**, 8579.

36. J. W. Steed, *Chem. Soc. Rev.,* 2010, **39**, 3686.

37. M. L. Muro-Small, J. Chen and A. J. McNeil, *Langmuir,* 2011, **27**, 13248.

38. M. Raynal and L. Bouteiller, *Chem. Commun.,* 2011, **47**, 8271.

39. J. Gao, S. Wu and M. A. Rogers, *J. Mater. Chem.,* 2012, **22**, 12651.

40. L. Meazza, J. A. Foster, K. Fucke, P. Metrangolo, G. Resnati and J. W. Steed, *Nat. Chem.,* 2013*,* **5,** 42.

41. D. M. Zurcher and A. J. McNeil, *J. Org. Chem.,* 2015*,* **80**, 2473.

42. R. Luboradzki, O. Gronwald, M. Ikeda, S. Shinkai and D. N. Reinhoudt, *Tetrahedron,* 2000, **56,** 9595.

43. G. R. Desiraju, *Angew. Chem., Int. Ed.,* 1995, **34**, 2311.

44. G. R. Desiraju, J. J. Vittal and A. Ramanan, *Crystal Engineering - A Textbook*; World Scientific: Singapore, 2011.

45. P. Dastidar, *Chem. Soc. Rev.,* 2008, **37**, 2699.

46. P. Sahoo, R. Sankolli, H. Y. Lee, S. R. Raghavan and P. Dastidar, *Chem. Eur. J.,* 2012, **18**, 8057.

47. U. K. Das, D. R. Trivedi, N. N. Adarsh and P. Dastidar, *J. Org. Chem.,* 2009, **74**, 7111.

48. M. K. Church, M. Maurer, F. E. R. Simons, C. Bindslev-Jensen, P. van Cauwenberge, J. Bousquet, S. T. Holgate and T. Zuberbier, *Allergy,* 2010, **65**, 459.

49. K. Weller, C. Ziege, P. Staubach, K. Brockow, F. Siebenhaar, K. Krause, S. Altrichter, M. K. Church and M. Maurer, *PLoS ONE,* 2011, **6***,* e23931.

50. S. R. Raghavan and B. H. Cipriano, *Gel Formation: Phase Diagrams Using Tabletop Rheology and Calorimetry* in Molecular Gels, edited by R. G. Weiss and P. Terech, Springer, Amsterdam, p.233 **(**2005**)**.

51. T. Mosmann, *Journal of Immunological Methods*, 1983, **65**, 55.

52. J. L. Garrigue, J. F. Nicolas, R. Fraginals, C. Benezra, H. Bour and D. Schmitt, *Contact Dermatitis,* 1994, **30**, 231.

53. E. Y. Zhang, A. Y. Chen and B. T. Zhu, *PLoS ONE,* 2009, **4,** e7703.

54. B. Young and J. H. Heath, *Wheater's Functional Histology - A Text and Colour Atlas;* 4th Edition, Harcourt Publishers Limited: London, 2000, pp157-171.

55. M. H. Kim, Y. Y. Choi, G. Yang, I.-H. Cho, D. Nam and W. M. Yang, *J. Ethnopharmacology*, 2013, **145**, 214.

56. Y. Seto, H. Nakajima, A. Suto, K. Shimoda, Y. Saito, K. I. Nakayama and I. Iwamoto*, J. Immunol.,* 2003, **170**, 1077.

Table of Contents (TOC) graphic:

The easiest reaction like salt formation has been exploited to design the first anti-allergic supramolecular topical gel capable of treating dinitrochlorobenzene (DNCB)–induced skin allergy of mice in self-delivery fashion.